A Stopping Radius for the Sphere Decoder: Complexity Reduction in Multiple–Symbol Differential Detection

Andreas Schenk and Robert F.H. Fischer
Lehrstuhl für Informationsübertragung, Universität Erlangen–Nürnberg, Erlangen, Germany

***Abstract*—With the aim of reducing its search complexity, we study a stopping radius for the sphere decoder (SD) algorithm. We compare two variants in setting this stopping radius. In particular, we consider a stopping radius, based on a lower bound on the packing radius, which preserves the optimality of the SD output, and a stopping radius which is based on the statistics of the underlying search problem. We adopt this SD with early termination to maximum-likelihood multiple-symbol differential detection (ML-MSDD) of differential phase-shift keying (DPSK), and compare the different stopping criteria in terms of achievable complexity reduction.**

I. Introduction

The sphere decoder (SD) is widely recognized as an efficient algorithm to solve maximum-likelihood (ML) detection problems in communications. See, e.g., [1] for ML-detection in multi-antenna systems, or [2] for ML multiple-symbol differential detection (MSDD) of differential phase-shift keying (DPSK) transmitted over time-varying fading channels.

There are different approaches to further reduce the SD complexity, most of which settled in the broad area of signal detection in multi-antenna systems. E.g., in [3], [4] a complexity reduction is achieved, at the cost of the decoders optimality, by statistical pruning of the underlying search tree. Although the approach in [5] preserves the SD optimality, the techniques introduced to reduce the number of SD search steps require solving complex optimization problems and thus significantly add to the overall decoder complexity.

In this paper, we aim to lower the number of SD search steps without sacrificing the optimality of the SD output using a simple technique, a recently introduced stopping radius for the SD [6]. Since this stopping radius is based on a lower bound on the so-called packing radius, it is possible to achieve a complexity reduction at preserved optimality of the SD output. In contrast to, e.g., [5], this termination criterion can be computed and integrated into the algorithm with negligible additional cost, and hence does not increase the overall SD complexity. We compare this adaptive, packing-radius-based stopping radius with a fixed stopping radius, based on the statistics of the underlying search problem.

We conduct this evaluation in the framework of ML detection of DPSK [2]. Here, for time-varying fading channels conventional symbol-by-symbol differential detection (DD) shows a significant loss in the bit error rate (BER) compared to coherent detection. This can be alleviated by ML-MSDD, i.e., the joint decision on a block of symbols. The SD stopping radius is adopted to this problem and its benefits in terms of reduced search complexity are verified via numerical results. However, it is noteworthy that this SD with early termination can be transfered to other applications as well (cf. e.g. [7]).

This work was supported by Deutsche Forschungsgemeinschaft (DFG) within the framework UKoLoS under grant FI 982/3-1.

This paper is outlined as follows. In Section II we describe the SD search process in the general framework of lattice decoding, and review how the stopping radius, based on the packing radius, does not alter the optimality of the decoder output. In Section III we sketch the formulation of the ML-MSDD problem of DPSK and adopt the SD stopping criterion to this setting. Numerical evidence for the achievable complexity reduction is provided in Section IV. A summary concludes the paper with Section V.

II. The Sphere Decoder with Early Termination

We first consider the general problem of finding the closest point in an L-dimensional discrete set

$$\mathbf{\Lambda} \stackrel{\text{def}}{=} \left\{ \boldsymbol{\lambda} = \boldsymbol{z}\boldsymbol{G} | \, \boldsymbol{z} \in \mathcal{Z}^L \right\} \tag{1}$$

with generator matrix $\boldsymbol{G} \in \mathbb{C}^{L\times L}$, and L-dimensional index set $\mathcal{Z}^L$, i.e., to find the member of $\mathbf{\Lambda}$ closest to a given $\boldsymbol{x} \in \mathbb{C}^L$:

$$\hat{\boldsymbol{\lambda}} = \underset{\boldsymbol{\lambda}\in\mathbf{\Lambda}}{\operatorname{argmin}} \|\boldsymbol{x} - \boldsymbol{\lambda}\|^2 \, . \tag{2}$$

Problem (2) arises, e.g., in lattice decoding, where $\mathcal{Z}^L = \mathbb{Z}^L$ [8], and in ML detection in multi-antenna systems, cf. e.g. [1]. In Section III we will recall how the special case of a shortest-vector problem, i.e., $\boldsymbol{x} = \boldsymbol{0}$ in (2), is related to ML-MSDD of DPSK [2].

A. SD Search Process

The SD is directly applicable to solve (2) if the generator matrix $\boldsymbol{G}$ has triangular structure. Since it is the most efficient search strategy, subsequently, we consider the SD applying the Schnorr–Euchner strategy with radius update [8]. The SD first finds the decision-feedback (DF) (or nearest-plane) point by substracting the contribution of already decided dimensions and rounding in every dimension l to the closest

$(l-1)$-dimensional hyperplane. The DF point is stored as a preliminary result and its distance to $\boldsymbol{x}$ serves as a search radius. To guarantee optimality, the SD now iteratively cycles through the next-best hyperplanes, checks if they lie in the search sphere, and updates the preliminary result and search radius, if a new point (hyperplane of dimension $l = 0$) is found within. If all hyperplanes in the search sphere have been checked and hence, no further points lie inside, the SD returns the last preliminary result, i.e., the closest point to $\boldsymbol{x}$ in $\boldsymbol{\Lambda}$.

B. Complexity Measure

The number of examined hyperplanes C (mean value $\overline{C}$) is equal to the number of examined tree nodes when viewing the SD search process in a tree of depth L. As suggested in [9], we adopt the logarithm to the base L of this figure, i.e., the complexity exponent $\log_L(\overline{C})$, as a measure for the expected SD complexity. In contrast to, e.g., the number of arithmetic operations or decoding time, this complexity measure is independent of the specific implementation of the SD (see, e.g., [10] for a very efficient implementation). However, it does not reflect the worst case complexity of the SD, which is always exponential in L [8].

C. Stopping Radius

The SD search process is terminated early for any preliminary point $\tilde{\boldsymbol{\lambda}}$, which is close enough to $\boldsymbol{x}$ with respect to a given stopping radius R_{stop}, i.e., if it satisfies

$$\|\tilde{\boldsymbol{\lambda}} - \boldsymbol{x}\|^2 \leq R_{\mathrm{stop}}^2 \, . \tag{3}$$

This $\tilde{\boldsymbol{\lambda}}$ is returned as the decoding result.

To preserve the optimality of the SD output, despite this early termination, we base this stopping radius on the packing radius [12, Appendix C]

$$\rho\left(\boldsymbol{\Lambda}\right) \stackrel{\mathrm{def}}{=} \frac{1}{2} \cdot \min_{\boldsymbol{\lambda},\boldsymbol{\lambda}' \in \boldsymbol{\Lambda}, \boldsymbol{\lambda} \neq \boldsymbol{\lambda}'} \|\boldsymbol{\lambda}' - \boldsymbol{\lambda}\| \tag{4}$$

of the underlying discrete set $\boldsymbol{\Lambda}$. Spheres of radius equal to the packing radius centered at each point of $\boldsymbol{\Lambda}$ are the largest inspheres of the *Voronoi regions*, the set of all points in $\mathbb{C}^L$ that are closer to $\boldsymbol{\lambda}$ than to any other member of $\boldsymbol{\Lambda}$, namely

$$\mathcal{R}_V(\boldsymbol{\lambda}) \stackrel{\mathrm{def}}{=} \left\{ \boldsymbol{x} \in \mathbb{C}^L \middle| \, \|\boldsymbol{x} - \boldsymbol{\lambda}\| \leq \|\boldsymbol{x} - \boldsymbol{\lambda}'\|, \forall \boldsymbol{\lambda}' \in \boldsymbol{\Lambda} \right\}. \tag{5}$$

See Figure 1 (dotted circles) for an illustration of a two dimensional lattice with its Voronoi regions (dashed gray). Any $\boldsymbol{\lambda}$ in the stopping sphere of radius $R_{\mathrm{stop}} = \rho\left(\boldsymbol{\Lambda}\right)$ centered at $\boldsymbol{x}$ is the closest point to $\boldsymbol{x}$ (Figure 1: x and full circle). (The converse does not hold.) Hence, the SD search process may be terminated without altering the optimality of the SD output.

Yet, for arbitrary $\boldsymbol{\Lambda}$ the packing radius is not known and equally hard to find as the closest point itself. However, a lower bound, which consequently still preserves optimality, is found from lattice reduction techniques [13]. For upper-triangular $\boldsymbol{G}$, the packing radius of $\boldsymbol{\Lambda}$ is lower bounded by [6]

$$\rho\left(\boldsymbol{\Lambda}\right) \geq R_\rho \stackrel{\mathrm{def}}{=} \frac{1}{2} \sqrt{d_{\min}^2\left(\mathcal{Z}\right)} \cdot \min_{i=1,\ldots,L} |g_{i,i}|. \tag{6}$$

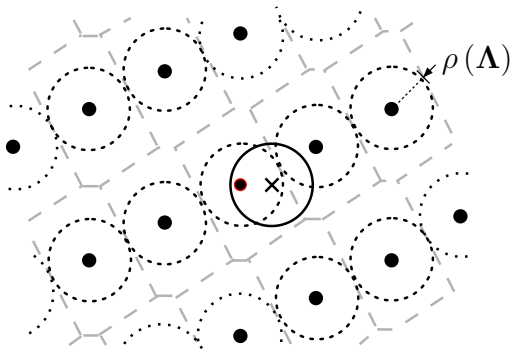

Fig. 1. Sketch of a two dimensional lattice to illustrate the meaning of the packing radius $\rho\left(\boldsymbol{\Lambda}\right)$ for closest-point-problems. Dots: Lattice points, dashed lines: Voronoi regions, dotted circles: circles of radius $\rho\left(\boldsymbol{\Lambda}\right)$ centered at the lattice points (incircles of the Voronoi regions), solid circle: circle of radius $\rho\left(\boldsymbol{\Lambda}\right)$ centered at $\boldsymbol{x}$, red: closest lattice point to $\boldsymbol{x}$.

See [6] for an extension to arbitrary $\boldsymbol{G}$, based on the orthogonal basis of $\boldsymbol{G}$.

We sketch the proof for upper-triangular $\boldsymbol{G}$. Let $\boldsymbol{z}, \boldsymbol{z}' \in \mathcal{Z}^L$, $\boldsymbol{z} \neq \boldsymbol{z}'$, be indices taken from an arbitrary index set $\mathcal{Z}$ of known minimum squared Euclidean distance

$$d_{\min}^2\left(\mathcal{Z}\right) \stackrel{\mathrm{def}}{=} \min_{z_i', z_i \in \mathcal{Z}, z_i' \neq z_i} |z_i' - z_i|^2 \, , \quad 1 \leq i \leq L \, , \tag{7}$$

Since $\boldsymbol{z}$ and $\boldsymbol{z}'$ differ at least in one position, the squared distance of the corresponding points of $\boldsymbol{\Lambda}$, $\boldsymbol{\lambda} = \boldsymbol{z}\boldsymbol{G}$, $\boldsymbol{\lambda}' = \boldsymbol{z}'\boldsymbol{G}$, satisfies

$$\begin{aligned} \|\boldsymbol{\lambda}' - \boldsymbol{\lambda}\|^2 &= \|(\boldsymbol{z}' - \boldsymbol{z})\boldsymbol{G}\|^2 \\ &= |z_1' - z_1|^2 \left(|g_{1,1}|^2 + \cdots + |g_{1,L}|^2\right) \\ &\quad + \cdots + |z_L' - z_L|^2 |g_{L,L}|^2 \\ &\geq d_{\min}^2\left(\mathcal{Z}\right) \cdot \min_{i=1,\ldots,L} |g_{i,i}|^2 \, . \end{aligned} \tag{8}$$

In combination with (4), this proofs the lower bound on the packing radius (6).

To account for a possible underestimation of the packing radius, we include a scaling factor $\alpha \geq 0$ for the packing-radius-based stopping radius and set

$$R_{\mathrm{stop}}^2 = \alpha \cdot R_\rho^2 \, . \tag{9}$$

Noteworthy, the computation of the packing-radius-based stopping criterion (multiplication of the minimum diagonal element of the generator matrix with the precalculated, minimum distance of the index set $\mathcal{Z}$) requires only low-complexity operations. Since the stopping radius adapts to the current search problem, $\alpha \leq 1$ clearly preserves the optimality of the decoder output. Enlarging the stopping radius with $\alpha \geq 1$ enables a trade-off between performance and complexity. The extreme cases $R_{\mathrm{stop}}^2 = 0$, i.e., $\alpha = 0$, and $R_{\mathrm{stop}}^2 \to \infty$, i.e., $\alpha \to \infty$, model the original SD without stopping radius and DF decoding, respectively, which serve as benchmark cases regarding complexity and performance.

An alternative way is to choose the stopping radius based on the expected distance of $\boldsymbol{x}$ to $\hat{\boldsymbol{\lambda}}$ [14], i.e.,

$$R_{\mathrm{stop}}^2 = \beta \cdot R_{\mathrm{E}}^2 \stackrel{\mathrm{def}}{=} \beta \cdot \mathrm{E}\{\|\hat{\boldsymbol{\lambda}} - \boldsymbol{x}\|^2\} \tag{10}$$

with a factor $\beta \geq 0$ for scaling. As this stopping radius does not adapt to the actual generator matrix, it does not preserve the optimality of the SD output. In Section IV we compare both strategies in the framework of MSDD of DPSK.

Noteworthy, the proposed stopping radius can be introduced in different SD search strategies, e.g., the Fincke–Phost search strategy, as well, and is easily combined with further techniques to reduce the SD search complexity, e.g., optimization of the initial SD search radius, limits to the worst-case complexity, and methods to fix the SD complexity [11].

III. MSDD OF DPSK USING THE SD

In this section we transfer the stopping radius to the SD applied in MSDD of DPSK transmitted over time-varying correlated Rayleigh fading channels. To this end, we first introduce the system model and review ML-MSDD and its formulation as a shortest-vector problem, making it applicable to be solved by the SD [2].

A. System Model

The sampled received signal of DPSK transmitted over a flat fading channel can be written as

$$r[i] = h[i]s[i] + n[i] \tag{11}$$

where the transmitted signal $s[i]$ is obtained from differential encoding of information symbols $a[i]$, i.e., $s[i] \stackrel{\text{def}}{=} a[i]s[i-1]$, $s[0] \stackrel{\text{def}}{=} 1$, i is the discrete time index, and $a[i], s[i]$ are M-PSK symbols, i.e., $a[i], s[i] \in \mathcal{M} \stackrel{\text{def}}{=} \left\{ \mathrm{e}^{\mathrm{j}\frac{2\pi}{M}m} | m = 0, 1, ..., M-1 \right\}$. $h[i]$ denotes the complex channel coefficient, and $n[i]$ is additive white circular symmetric complex Gaussian noise of variance N_0/T, with the one-sided power spectral density N_0, and symbol duration T. The signal-to-noise ratio (SNR) in dB reads $10\log(E_\mathrm{b}/N_0)$, with the energy per bit $E_\mathrm{b} = 1/\log_2(M)$.

As in [2], [15], we consider a correlated time-varying channel according to Clarke's fading model, i.e., $\mathrm{E}\{h[i+\kappa]h^*[i]\} = J_0(2\pi B_\mathrm{f} T\kappa)$, where $J_0(\cdot)$ denotes the zeroth order Bessel function of first kind, and $B_\mathrm{f}T$ the normalized maximum fading bandwidth.

B. MSDD Decision Metric

It is known that symbol-by-symbol DD suffers from an error floor in the BER curves for time-varying fading channels, i.e., $B_\mathrm{f}T > 0$. This can be alleviated by ML-MSDD, which performs a joint decision of L information symbols based on a block $\boldsymbol{r} \stackrel{\text{def}}{=} [r[0], ..., r[N-1]]$ of N receive symbols, where $N \stackrel{\text{def}}{=} L+1$ denotes the MSDD window length (w.l.o.g. we consider the block starting at $i = 0$), cf. e.g. [15]. Translating (11) to a vectorized model results in

$$\boldsymbol{r} = \boldsymbol{h}\mathrm{diag}(\boldsymbol{s}) + \boldsymbol{n} \tag{12}$$

with $\boldsymbol{s} \stackrel{\text{def}}{=} [s[0], ..., s[L]] \in \mathcal{M}^N$, and similar definitions for $\boldsymbol{h}$ and $\boldsymbol{n}$. The ML estimate of the transmit signal $\hat{\boldsymbol{s}} \in \mathcal{M}^N$ is the trial sequence $\tilde{\boldsymbol{s}} \in \mathcal{M}^N$ that maximizes the probability density function evaluated at the receive signal vector, i.e., for the case of Gaussian noise,

$$\hat{\boldsymbol{s}} = \underset{\substack{\tilde{\boldsymbol{s}} \in \mathcal{M}^N \\ \tilde{s}_0 = 1}}{\mathrm{argmax}} \frac{1}{\pi^N \det \boldsymbol{\Phi}_{\boldsymbol{r}\boldsymbol{r}|\tilde{\boldsymbol{s}}}} \mathrm{e}^{-\boldsymbol{r}\boldsymbol{\Phi}_{\boldsymbol{r}\boldsymbol{r}|\tilde{\boldsymbol{s}}}^{-1}\boldsymbol{r}^\mathsf{H}} \tag{13}$$

with $\boldsymbol{\Phi}_{\boldsymbol{r}\boldsymbol{r}|\tilde{\boldsymbol{s}}} \stackrel{\text{def}}{=} \mathrm{E}\{\boldsymbol{r}^\mathsf{H}\boldsymbol{r}|\tilde{\boldsymbol{s}}\}$. Since we assume white noise, $\boldsymbol{\Phi}_{\boldsymbol{r}\boldsymbol{r}|\tilde{\boldsymbol{s}}} = \mathrm{diag}(\tilde{\boldsymbol{s}})\boldsymbol{C}\mathrm{diag}(\tilde{\boldsymbol{s}})^\mathsf{H}$, with the channel correlation matrix $\boldsymbol{C} \stackrel{\text{def}}{=} \mathrm{E}\{\boldsymbol{h}^\mathsf{H}\boldsymbol{h}\} + \frac{N_0}{T}\boldsymbol{I}_N$.

As shown in [2], applying the Cholesky factorization to the inverse of the channel correlation matrix, i.e., $\boldsymbol{C}^{-1} = \boldsymbol{U}\boldsymbol{U}^\mathsf{H}$, (13) can be reformulated to

$$\hat{\boldsymbol{s}} = \underset{\substack{\tilde{\boldsymbol{s}} \in \mathcal{M}^N \\ \tilde{s}_0 = 1}}{\mathrm{argmin}} \|\tilde{\boldsymbol{s}}\boldsymbol{G}\|^2, \tag{14}$$

where $\boldsymbol{G} \stackrel{\text{def}}{=} (\mathrm{diag}(\boldsymbol{r})\boldsymbol{U})^*$ is an N-dimensional upper-triangular matrix.

C. Transfer of Stopping Radius

It can readily be seen that (14) is equivalent to a shortest vector problem in an N-dimensional discrete set

$$\boldsymbol{\Lambda} \stackrel{\text{def}}{=} \left\{ \boldsymbol{\lambda} = \tilde{\boldsymbol{s}}\boldsymbol{G} | \, \tilde{\boldsymbol{s}} \in \mathcal{M}^N, \tilde{s}_0 = 1 \right\} \tag{15}$$

with generator matrix $\boldsymbol{G}$ and "indices" $\tilde{\boldsymbol{s}}$. Since the first component is fixed due to the differential encoding, its fixed contribution may be substracted, and the dimensionality of the search process is reduced to $L = N - 1$. Consequently, we adopt the stopping criterion and terminate the SD search process for any $\tilde{\boldsymbol{s}}$ fulfilling

$$\|\tilde{\boldsymbol{s}}\boldsymbol{G}\|^2 - |g_{0,0}|^2 \leq R_\mathrm{stop}^2 \, . \tag{16}$$

The minimum distance of the index set $\mathcal{M}$, see (7), is found to be $d_\mathrm{min}^2(\mathcal{M}) = 4\sin^2\left(\frac{\pi}{M}\right)$. Hence, from (6) a lower bound on the packing radius is given by

$$R_\rho^2 = \sin^2\left(\frac{\pi}{M}\right) \cdot \min_{i=1,...,L} |g_{i,i}|^2 \tag{17}$$

Together with the scaling factor α, this yields a stopping radius for the SD in MSDD of DPSK

$$R_\mathrm{stop}^2 = \alpha \cdot R_\rho^2 \tag{18}$$

which is easy to compute and for $\alpha \leq 1$ guarantees the ML property of the estimated sequence.

Figure 2 depicts the dependecy of the lower bound on the SNR for DQPSK ($M = 4$) and MSDD window length $L = 3, 5, 9, 14$ at $B_\mathrm{f}T = 0.01$ (left) and $B_\mathrm{f}T = 0.03$ (right). The average decision metric of the ML sequence, $R^2 \stackrel{\text{def}}{=} \|\boldsymbol{s}\boldsymbol{G}\|^2 - |g_{0,0}|^2$, is included for comparison. Especially for $B_\mathrm{f}T = 0.01$, R_ρ^2 grows rapidly with increasing SNR. We conclude that the ML point lies inside the circle of radius R_ρ already at low SNR, indicating its practical use as a stopping radius.

To illustrate this behaviour, we restrict to real signals, $L = 2$, and binary DPSK with $M = 2$, yielding $d_\mathrm{min}(\mathcal{M}) = 2$. Figure 3 shows a typical realization of the set $\boldsymbol{\Lambda}$ in the $(\tilde{s}_0 = 1)$-plane for low and high SNR and $B_\mathrm{f}T = 0.01$. Each of the four trial sequences corresponds to one point of $\boldsymbol{\Lambda}$. The

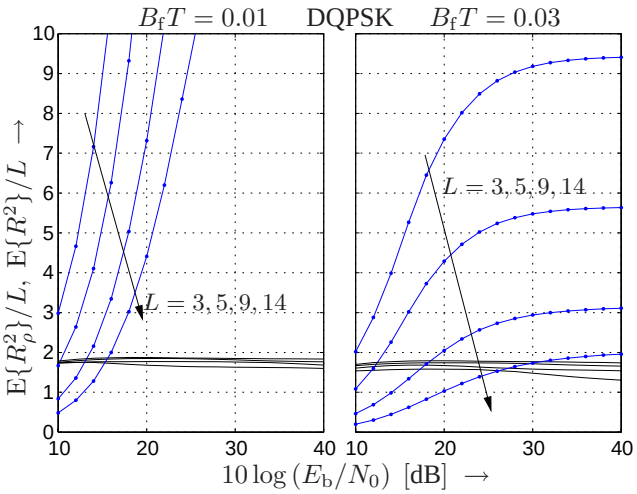

Fig. 2. Average stopping radius $\mathrm{E}\{R_\rho^2\}$ (blue) vs. E_b/N_0 in [dB] in comparison to the average final ML-MSDD metric $\mathrm{E}\{R\}$ (black), both normalized to L, of MSDD with $L = 3, 5, 9, 14$ (R_ρ: top to bottom, R: reverse) for DQPSK ($M = 4$).

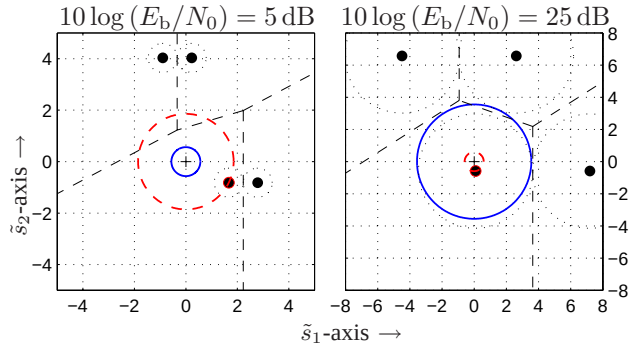

Fig. 3. A typical realization of the set $\mathbf{\Lambda}$ in the $(\tilde{s}_0 = 1)$-plane underlying the SD search in MSDD with $L = 2$, $M = 2$, and $B_\mathrm{f}T = 0.01$. Solid blue circle: stopping radius R_ρ centered at $\mathbf{0}$, red: ML estimate and corresponding circle centered at $\mathbf{0}$, dashed lines: Voronoi regions, dotted black: circles of radius R_ρ centered at the points of $\mathbf{\Lambda}$.

ML-MSDD result, the point of $\mathbf{\Lambda}$ closest to the origin, together with its corresponding circle of radius R centered at the origin is depicted with a dashed red line. A solid blue circle with radius $R_\mathrm{stop} = R_\rho = \min_{i=1,2}|g_{i,i}|$ represents the stopping radius. One observes, that $2R_\rho$ is equal to the minimum distance of the four points in $\tilde{s}_1$ and $\tilde{s}_2$ direction. Note the similarity to the closest-point-problem of lattices (cf. Figure 1) and the hereby motivated choice for R_ρ.

Independent of the SNR, the length of the shortest vector stays in the same order, but the minimum distance of two points of $\mathbf{\Lambda}$, and hence the packing radius, increases rapidly with increasing SNR. At low SNR two points are very close to each other, their decision metrics—the distance to origin—differ insignificantly. Consequently, on the one hand the decision is not very reliable, and on the other hand the packing radius of $\mathbf{\Lambda}$ is dominated by these two points. Hence, the stopping criterion is not met, although the estimate of $\rho(\mathbf{\Lambda})$ is relatively good. With increasing SNR, $\rho(\mathbf{\Lambda})$ grows rapidly—three of the four points move away form the origin—, yielding on the one hand a more reliable decision and on the other hand an increased packing radius.

In light of Figure 2, we refrain from exactly evaluating (10) to find a stopping radius based on the expected decision metric. It can be seen that the average decision metric of the ML sequence varies only little for different maximum normalized fading bandwidths $B_\mathrm{f}T$ and is approximately linear in L, independent of the SNR. Hence, we fix

$$R_\mathrm{stop}^2 = \beta \cdot L \tag{19}$$

with a factor $\beta \geq 0$ for scaling. This setting of the fixed stopping radius is also supported by the fact that the decision metric of the true transmitted sequence, $\|\boldsymbol{s}\boldsymbol{G}\|^2$, is χ^2 distributed with mean $L + 1$ [16].

IV. Numerical Results

We compare the different strategies in setting the stopping radius for the SD via numerical results in terms of power efficiency, i.e., the required SNR to guarantee a certain BER, and in terms of average decoder complexity. We adopt the complexity exponent as a measure for the SD complexity, cf. Section II-B. ML-MSDD, as achieved by the original SD without early termination, and DF-DD serve as the benchmark cases.

Figure 4 depicts the BER performance of MSDD of DQPSK ($M = 4$) using the SD with different stopping radii in comparison to DF-DD (i.e., $R_\mathrm{stop}^2 \rightarrow \infty$, dashed gray line), conventional symbol-by-symbol DD, and coherent detection with perfect channel knowledge. It can be seen that the packing-radius-based stopping radius R_ρ^2 (dashed blue with markers) achieves exactly ML-MSDD performance (solid red) obtained with the tradional SD without stopping radius. The constant stopping radius $R_\mathrm{stop}^2 = 1.5L$ (dashed green) shows some loss compared to ML-MSDD.

However, from Figure 5, and similar for 8-DPSK in Figure 6, we observe that the use of the stopping radius R_ρ^2 significantly reduces the complexity exponent. As expected from Figure 2 and Figure 3, this reduction is pronounced for $B_\mathrm{f}T = 0.01$ and moderate to high SNR. In this regime, the dominant event in the traditional SD search is to find the DF point and then to check a single alternative in every dimension, which is rejected due to the updated search radius. The former involves the visit of L hyperplanes, while the latter contributes another $L - 1$ search steps. Hence, the expected complexity exponent approaches $\log_L(2L-1)$. With the proposed stopping radius, often the DF point lies inside the sphere of radius $R_\mathrm{stop} = R_\rho$, and the search terminates after visiting L hyperplanes. Thus, in many cases the DF-DD result already is identified as the ML-MSDD, which results in a reduced complexity exponent of $\log_L(L) = 1$.

The fixed stopping radius $R_\mathrm{stop}^2 = 1.5L$ mainly strikes at low SNR and has little effect at high SNR.

Scaling factors α and β have been introduced to relax the stopping criterion. Clearly $\alpha = \beta = 0$ corresponds to the traditional SD, and $\alpha = \beta \rightarrow \infty$ to DF-DD. Figure 7 depicts the resulting trade-off of power efficiency against complexity

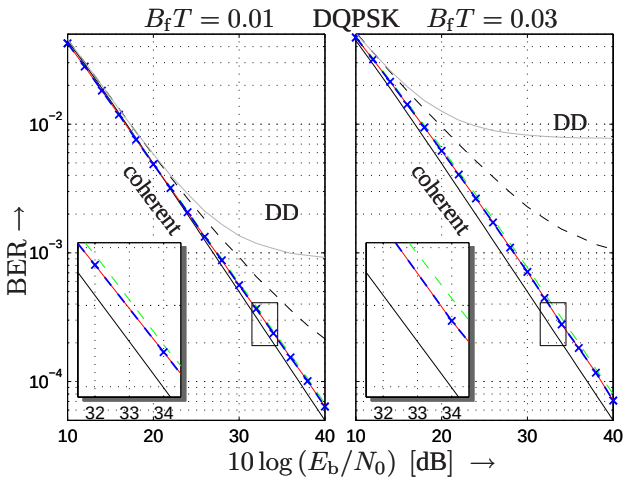

Fig. 4. BER vs. E_b/N_0 in [dB] of MSDD using the original SD ($R^2_\mathrm{stop} = 0$, solid red line), the SD with optimum stopping radius ($R^2_\mathrm{stop} = R^2_\rho$, dashed blue with markers), and the SD with $R^2_\mathrm{stop} = 1.5L$ (dashed green) for $L = 14$ in comparison to DF-DD (dashed black), DD, and coherent detection at $B_\mathrm{f}T = 0.01$ (left) and $B_\mathrm{f}T = 0.03$ (right) for DQPSK ($M = 4$).

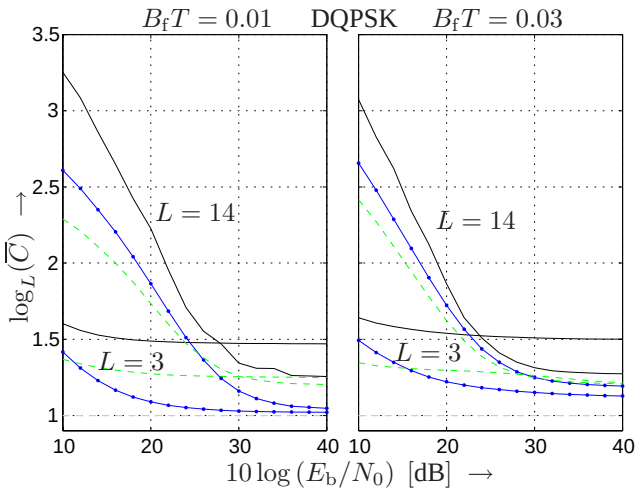

Fig. 5. Average complexity exponent vs. E_b/N_0 in [dB] of MSDD using the original SD ($R^2_\mathrm{stop} = 0$, solid black line), the SD with optimum stopping radius ($R^2_\mathrm{stop} = R^2_\rho$, blue), and the SD with $R^2_\mathrm{stop} = 1.5 \cdot L$ (dashed green) for $L = 3$ and $L = 14$ in comparison to DF-DD (dashed black) at $B_\mathrm{f}T = 0.01$ (left) and $B_\mathrm{f}T = 0.03$ (right) for DQPSK ($M = 4$).

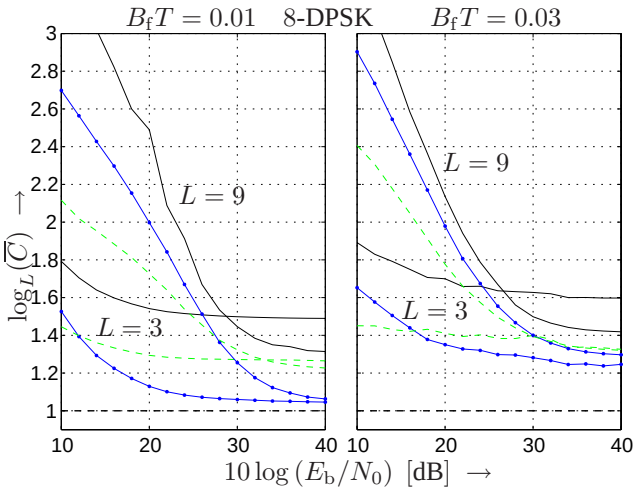

Fig. 6. Average complexity exponent vs. E_b/N_0 in [dB] of MSDD using the original SD ($R^2_\mathrm{stop} = 0$, solid black line), the SD with optimum stopping radius ($R^2_\mathrm{stop} = R^2_\rho$, blue), and the SD with $R^2_\mathrm{stop} = 1.5 \cdot L$ (dashed green) for $L = 3$ and $L = 9$ in comparison to DF-DD (dashed black) at $B_\mathrm{f}T = 0.01$ for 8-DPSK ($M = 8$).

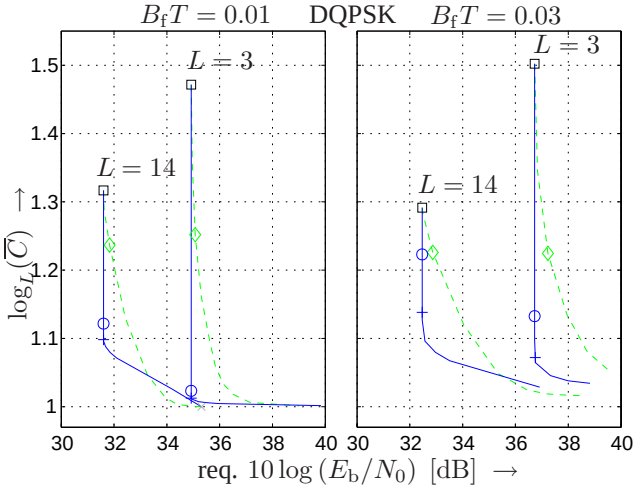

Fig. 7. Trade-off between power efficiency and complexity at BER $= 4 \cdot 10^{-4}$ of MSDD with $N = 4$ and $N = 15$ at $B_\mathrm{f}T = 0.01$ (left) and $B_\mathrm{f}T = 0.03$ (right) for DQPSK ($M = 4$). Curves are parameterized by α (solid blue), β (dashed green). Black square marker: $\alpha = \beta = 0$, traditional SD, blue circle: $\alpha = 1$, $R^2_\mathrm{stop} = R^2_\rho$, blue cross: $\alpha = 4$, $R^2_\mathrm{stop} = 4 \cdot R^2_\rho$, green diamond: $R^2_\mathrm{stop} = 1.5L$.

between these two extreme cases for $L = 3$ and $L = 14$ at BER $= 4 \cdot 10^{-4}$ achieved with the parameters α and β. In particular, $\alpha = 1$, i.e., $R^2_\mathrm{stop} = R^2_\rho$ guarantees optimality. Interestingly, an increase up to $\alpha \approx 4$ does not alter the optimality. This is a result of the underestimation of the packing radius [6]. Note that DF-DD does not always achieve the desired BER, hence, the minimum complexity of DF-DD can not be reached and the trade-off curves end before.

Although a complexity reduction is also achieved with the fixed stopping radius (the diamond marks $\beta = 1.5$, i.e., $R^2_\mathrm{stop} = 1.5L$), there is a significant loss in power efficiency as β increases.

Figure 8 summarizes these results for different L at BER $= 10^{-2}$, BER $= 10^{-3}$, and BER $= 2 \cdot 10^{-4}$. At each L and BER the trade-off curves similar to Figure 7 are shown. For better illustration, the corresponding points of $R^2_\mathrm{stop} = R^2_\rho$ ($\alpha = 1$), $R^2_\mathrm{stop} = 1.5L$, the original SD, and DF-DD of different L are connected by solid lines (blue, green, black, and gray, respectively). Their projections on the ground plain are depicted as dashed lines.

We observe that increasing L reduces the required SNR to achieve a similar BER, with most of the gain achieved already for moderate L. The proposed, adaptive stopping radius is clearly superior in terms of complextiy and power efficiency for $B_\mathrm{f}T = 0.01$ and at low BER. The fixed stopping radius has some complexity advantage at large BER, however this reduction is only achieved at a decreased power efficiency.

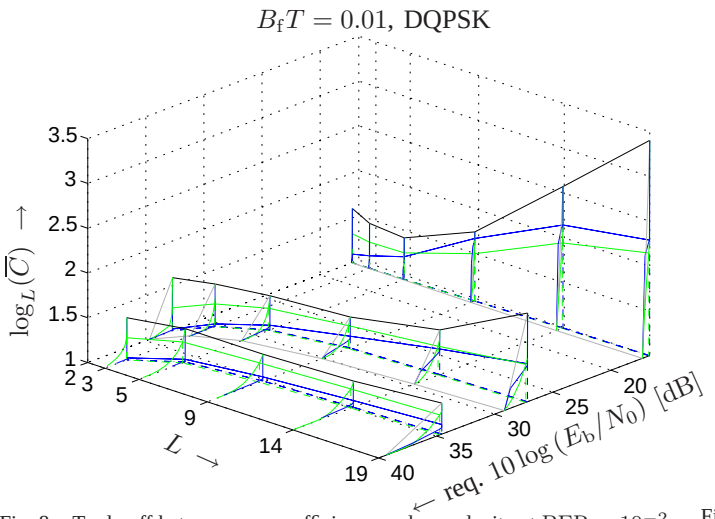

Fig. 8. Trade-off between power efficiency and complexity at $\mathrm{BER} = 10^{-2}$ (back), $\mathrm{BER} = 10^{-3}$ (middle), $\mathrm{BER} = 2 \cdot 10^{-4}$ (front) at different L at $B_\mathrm{f}T = 0.01$ for DQPSK ($M = 4$). $R^2_\mathrm{stop} = R^2_\rho$ ($\alpha = 1$), $R^2_\mathrm{stop} = 1.5L$, the original SD, and DF-DD of different L are connected by solid lines (blue, green, black, and gray, respectively, projection to ground: dashed lines).

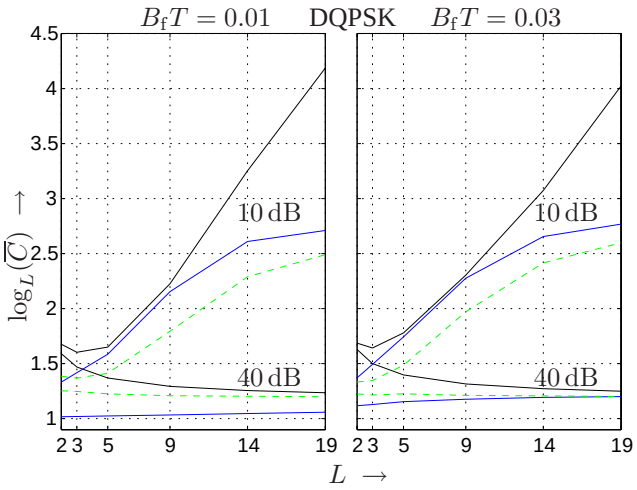

Fig. 9. Average complexity exponent vs. MSDD parameter L at $10\log(E_\mathrm{b}/N_0) = 10\,\mathrm{dB}$ (top curves) and $10\log(E_\mathrm{b}/N_0) = 40\,\mathrm{dB}$ (bottom) at $B_\mathrm{f}T = 0.01$ (left) and $B_\mathrm{f}T = 0.03$ (right) for DQPSK ($M = 4$). Solid blue: $R^2_\mathrm{stop} = R^2_\rho$, dashed green: $R^2_\mathrm{stop} = 1.5L$, solid black: original SD.

Figure 9 highlights another effect also observed in Figure 8. The average complexity exponent over the MSDD parameter L at low and high SNR ($10\log(E_\mathrm{b}/N_0) = 10\,\mathrm{dB}$ and $10\log(E_\mathrm{b}/N_0) = 40\,\mathrm{dB}$, respectively) is shown. In addition to the already described complexity reduction at high SNR, we observe a significant drop of the complexity exponent for low SNR as well. While in this regime the complexity exponent of the original SD grows like $L/\log(L)$, i.e., shows a search complexity exponential in L [9], with the proposed stopping radii the complexity exponent grows considerably slower. Since the fixed and the adaptive stopping radius with this respect show similar behaviour, the latter is clearly favorable, as it achieves this complexity reduction without altering the optimality of the decoder output.

V. Conclusions

In this paper we have reviewed stopping criteria for the SD, with the aim of terminating the search process as early as possible, and thus reducing its complexity. Since this stopping criterion, we recently introduced, is based on a lower bound on the packing radius of discrete sets, our approach is able to achieve a complexity reduction without sacrificing optimality of the decoder output. We have illustrated the benefits of our adaptive, packing-radius-based stopping radius over a fixed stopping radius for ML-MSDD of DPSK and could observe a significant complexity reduction over a wide range of SNR. We note that the proposed termination criterion can be applied to different SD search strategies, and is easily combined with further techniques to reduce the SD search complexity, e.g., optimization of the initial SD search radius, limits to the worst-case complexity, and methods to fix the SD complexity.

References

[1] M. Damen, H. El Gamal, and G. Caire, "On Maximum-Likelihood Detection and the Search for the Closest Lattice Point," *IEEE Trans. Inf. Theory*, vol. 49, no. 10, pp. 2389–2402, Oct. 2003.

[2] L. Lampe, R. Schober, V. Pauli, and C. Windpassinger, "Multiple-Symbol Differential Sphere Decoding," *IEEE Trans. Commun.*, vol. 53, no. 12, pp. 1981–1985, Dec. 2005.

[3] R. Gowaikar and B. Hassibi, "Statistical Pruning for Near-Maximum Likelihood Decoding," *IEEE Trans. Signal Process.*, vol. 55, no. 6, pp. 2661–2675, Jun. 2007.

[4] A. Ghaderipoor and C. Tellambura, "A Statistical Pruning Strategy for Schnorr-Euchner Sphere Decoding," *IEEE Commun. Lett.*, vol. 12, no. 2, pp. 121–123, Feb. 2008.

[5] M. Stojnic, H. Vikalo, and B. Hassibi, "Speeding up the Sphere Decoder with H^∞ and SDP Inspired Lower Bounds," *IEEE Trans. Signal Process.*, vol. 56, no. 2, pp. 712–726, Feb. 2008.

[6] A. Schenk, R. F. H. Fischer, and L. Lampe, "A Stopping Radius for the Sphere Decoder and its Application to MSDD of DPSK," *Communications Letters, IEEE*, vol. 13, no. 7, pp. 465–467, Jul. 2009.

[7] ——, "A New Stopping Criterion for the Sphere Decoder in UWB Impulse-Radio Multiple-Symbol Differential Detection," in *2009 IEEE International Conference on Ultra-Wideband*, pp. 589–594, Vancouver, Canada, Sep. 2009.

[8] E. Agrell, T. Eriksson, E. Vardy, and K. Zeger, "Closest Point Search in Lattices," *IEEE Trans. Inf. Theory*, vol. 48, pp. 2201–2214, 2002.

[9] B. Hassibi and H. Vikalo, "On the Sphere-Decoding Algorithm I. Expected Complexity," *IEEE Trans. Signal Process.*, vol. 53, no. 8, pp. 2806–2818, Aug. 2005.

[10] A. Ghasemmehdi and E. Agrell, "Optimal Projection Method in Sphere Decoding," Jun 2009. [Online]. Available: http://arxiv.org/abs/0906.0249

[11] L. G. Barbero and J. S. Thompson, "Fixing the Complexity of the Sphere Decoder for MIMO Detection," *IEEE Trans. Wireless Commun.*, vol. 7, no. 6, pp. 2131–2142, Jun. 2008.

[12] R. F. H. Fischer, *Precoding and Signal Shaping for Digital Transmission*. New York, NY, USA: John Wiley & Sons, Inc., 2002.

[13] J. Von Zur Gathen and J. Gerhard, *Modern Computer Algebra*. New York, NY, USA: Cambridge University Press, 2003.

[14] Z. Guo and P. Nilsson, "Reduced Complexity Schnorr-Euchner Decoding Algorithms for MIMO Systems," *IEEE Commun. Lett.*, vol. 8, no. 5, pp. 286–288, May 2004.

[15] P. Ho and D. Fung, "Error Performance of Multiple-Symbol Differential Detection of PSK Signals Transmitted over Correlated Rayleigh Fading Channels," *IEEE Trans. Commun.*, vol. 40, no. 10, pp. 1566–1569, Oct. 1992.

[16] V. Pauli and L. Lampe, "On the Complexity of Sphere Decoding for Differential Detection," *IEEE Trans. Inf. Theory*, vol. 53, no. 4, pp. 1595–1603, Apr. 2007.